Deconvolution of soot particle size distributions

H. Mätzing*, P. Vlavakis, M. Sentko**, A. Loukou**, B. Stelzner**, D. Trimis** and D. Stapf***
corresponding author e-mail: hartmut.maetzing@kit.edu
*KIT, Institute for Technical Chemistry (ITC), D-76344 Eggenstein-Leopoldshafen, Germany
**KIT, Engler-Bunte-Institute (EBI-VBT), D-76131 Karlsruhe, Germany

Abstract
Soot particle size distributions are usually reported in single mode form which may be a crude approximation to the measurements. In this paper, soot particle size distributions were measured in premixed $CH_4/O_2/Ar$ flames by SMPS. Up to five lognormal modes were fitted to the experimental results by nonlinear least squares regression. The multimode size distributions give a much better representation of the experimental data than single mode size distributions. Fitting 1 – 3 peaks to the size distributions increases the accuracy of data representation, while fitting more peaks does not optimize the precision further. The data fits include some extrapolation beyond the size limits of the experimental data ($d_P \approx 5$ - 60 nm). This type of data evaluation was performed for measurements at several heights above the burner. With increasing height above the burner, peaks with large modal particle diameters are found to become more and more important, while the peak widths are close to the limit of self-preserving distributions. This report appears to be the first attempt to examine measured soot particle size distributions with ultimate precision. The technique allows representing the evolution of different particle modes as well as the evolution of the soot volume fractions in these modes. Future perspectives are to obtain more insight into the coagulation kinetics of soot particles.

Introduction
The production of high purity syngas during the partial oxidation of methane has been studied for many years [1,2]. It requires high equivalence ratios and, flame stabilization is achieved by enhanced flame temperatures (preheated feed gas, little N_2 or Ar). Under such oxy-fuel conditions, flame temperatures are often found to be superadiabatic [3,4]. The soot formation in such flames has been studied recently using an SMPS technique [5]. The standard data evaluation implies a single peak representation of the measured particle size distributions. However, the results obtained for these flames clearly indicate the presence of several particle modes superimposing each other. As a follow-up to the aforementioned work, the present data evaluation focuses particularly on the multimode nature of these size distributions. This novel post processing of the measured particle size distributions is not contradictory to the previous evaluation [5], rather it gives extended, supplementary information about the soot formation in these flames.

There are numerous reports on soot particle size distributions measured in flat flames. Dual mode size distributions have been detected by mass spectrometry recently and have been characterized quantitatively [6]. SMPS techniques have also been reported frequently [e.g. 7-9]. By visual inspection, the SMPS results often show (or at least indicate) the presence of several peaks, either because they have a distinctive global minimum or just because they look distorted. Some authors fitted two superimposed lognormal distributions to their experimental results [9,10], however, until so far, there have been no attempts to investigate the multimodal nature of such soot particle size distributions in detail.
In this paper, up to five lognormal modes are fitted to the measured particle size distributions using the method of nonlinear least squares regression by Differential Evolution (DE). In this way, it is possible to monitor the history of various particle modes and to investigate the evolution of the soot volume fractions in these modes.

Theory
Soot particle size distributions are represented by lognormal distributions usually. If this assumption is accepted for all individual modes of multimode distributions also, the deconvolution can be a laborious task, because it requires a nonlinear regression. Previous deconvolution methods are listed in [11] and recently, it has been shown that Differential Evolution (DE) is a powerful and fast method to perform this type of peak deconvolution [11]. Lognormal size distributions are characterized by three parameters, the modal diameter d_{P0}, the total number density N_0 and the distribution width log σ_g (or ln σ_g) and here, a summation is performed over 1 … imax distributions:

$$\frac{d\,N}{dlog\,d_P} = \sum_{i=1}^{imax} \frac{N_{0,i}}{\sqrt{2\,\pi}\cdot log\,\sigma_{g,i}} \cdot\ exp\left\{-\,0.5\ \cdot\ \frac{log^2\,d_P/\,d_{P0,i}}{log^2\,\sigma_{g,i}}\right\} \qquad (1)$$

The soot volume fractions $f_{v,i}$ of each peak are calculated from the third moments of the number distributions [12]:

$$f_{v,i} = \frac{1}{6}\pi\ N_{0,i}\ \cdot d_{P0,i}^{3}\ \cdot exp(ln^2 10\ \cdot\ {}^{9}/_{2}\ \cdot log^2\ \sigma_{g,i}) \qquad (2)$$

The DE fitting process starts with two arbitrary (random) population vectors for the provided diameters, generates a mutant vector therefrom and mixes the parameters of a mutant and a solution vector to obtain trial populations. Depending on fit quality, the trial solution is accepted or rejected and the iteration starts again until successive solutions converge and predefined quality criteria are reached (minimum sum of squared errors etc.). In this way, good fits to both differentiable and discontinuous functions can be obtained comparatively fast [13,14].
In this work, the F77 code provided by Mishra [15] was adapted to the problem type considered here. The final code, Fit4LogNorms, provides an interactive user

interface for data input and output. Input values are the particle diameters d_P [nm or µm], the measured number densities d N/dlog d_P [cm^{-3} or m^{-3}] and several control parameters, e.g.

- the numerical ranges within which to search d_{P0}, N_0 and log σ_g
- minimum required differences between adjacent peaks (ΔN_0, Δd_{P0} and Δlog σ_g); they are used to detect occasional peak identities.

Fit4LogNorms was tested against literature data [11] and against additional artificial test cases. In particular, Fit4LogNorms was found to give reliable results for incomplete (truncated) size distributions, as they are often found experimentally due to instrumental or other limitations [7-11]. Special care was taken for the treatment of sparse datasets which have not a sufficient number of data points to perform a reliable fit. In these cases, Fit4LogNorms offers the possibility to enlarge the sample size by Bezier interpolation. As described above, the fitting procedure is a purely mathematical tool and, it does not imply any assumptions about the physical processes behind (soot mass growth, particle coagulation).

Experimental

The measurements are part of a larger project described elsewhere [5], investigating the soot formation in fuel-rich methane flames at constant equivalence ratio Φ = 2.6, but at different temperatures. Here we report only results for the coldest flame (x_{CH4} = 0.342, x_{O2} = 0.264, x_{Ar} = 0.394). The flame was stabilized on a 30 mm i.d. heat-flux burner with a burner plate temperature of 160 °C. The cold gas velocity was 11.1 cm/sec (corresponding to the flame velocity as derived by the heat-flux burner method [3]) and the flame was not shielded against surrounding air. The flame temperatures were measured with an S-type (Pt–Rh) thermocouple (wire thickness 100 µm) and corrected for radiation losses. The accuracy is better than ± 200 K [5]. Soot sampling and instant dilution were performed along the central flame axis through the pinhole of a stainless steel pipe. Size measurements were performed with an SMPS system (TSI model 3938) which was operated with a soft X-ray Neutralizer (TSI model 3088), a nano DMA (TSI model 3085A) and a condensation particle counter (CPC, TSI model 3776). In a standard procedure, the total number density and the soot volume fraction were obtained by summing up over all size intervals Δlog d_P. The resulting data have been corrected for flame dilution and for diffusion losses in the transport line from the probe orifice until the SMPS inlet and within the SMPS system [5]. The evaluated median particle diameter divides the size distribution into two halves of 0.5 ΣN_i.

Results and Discussion

According to the previous standard data evaluation, the average size d_P of the soot particles and the soot volume fraction f_v were found to increase with increasing height above the burner (HAB), while the total soot particle number density was decreasing [5]. These findings are confirmed by the present data evaluation and, for the particular flame (at Φ = 2.6), the extended data evaluation is demonstrated here.

The flame and its temperature profile are shown in Figs. 1 and 2. Close to the main reaction zone, the maximum temperature was ~ 1950 K, which is ~ 250 K above the adiabatic value [3,4].

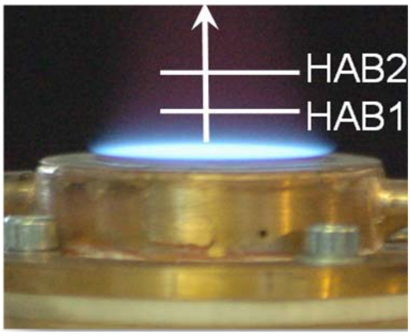

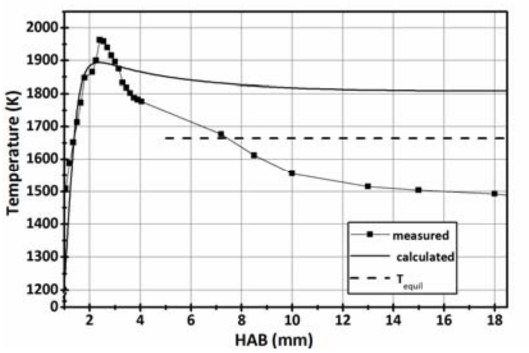

Figure 1. Heat-flux burner, sooting flame. **Figure 2.** Flame temperature profile.

Fig. 3 shows measured and fitted size distributions at HAB = 10 mm. The single peak fit does not represent the data points precisely. The triple peak fit represents the data points much better and, it extrapolates into the very small size range, beyond the limit of reliable measurements [5]. A particle inception mode around $d_P \approx 2$ nm is not unlikely at high flame temperatures [6,16]. With increasing peak number, the sum of squared errors decreases (Fig. 4), hence the fit quality is improved. The same fitting procedure was performed at several HAB. At low HAB, the resulting total particle number density is higher than the SMPS result because of the extrapolation mentioned above (Fig. 3). The coagulation rate constants of the coagulation modes are in the range $d(1/N)/dt = 6 - 12 \cdot 10^{-9}$ cm^3/sec, which is reasonable. A comparison of the particle size as determined by the SMPS and by the fitting procedure is shown in Fig. 5. The size distribution widths are in the range $\log \sigma_g = 0.15 - 0.19$, close to the self-preserving limit (~ 0.13). The total soot volume fractions differ by up to ± 30% (Fig. 6). This is

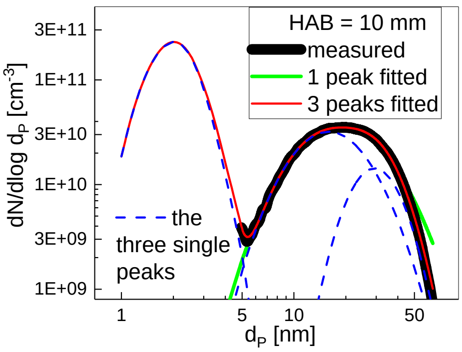

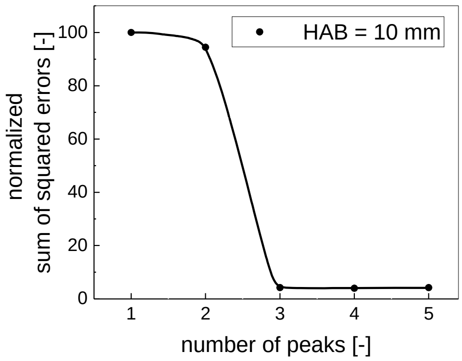

Figure 3. Three peak fitting example. **Figure 4.** Fit error vs. peak number.

because at low HAB, the peak fits give a smaller amount of large particles, while at high HAB, they give larger particle sizes.

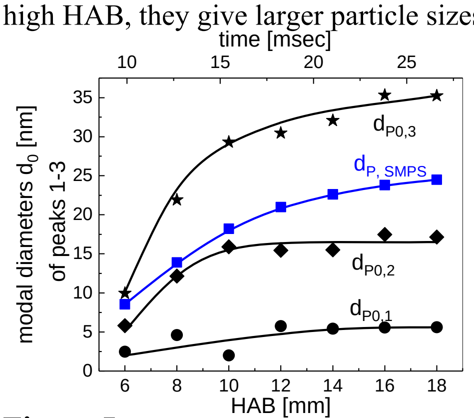

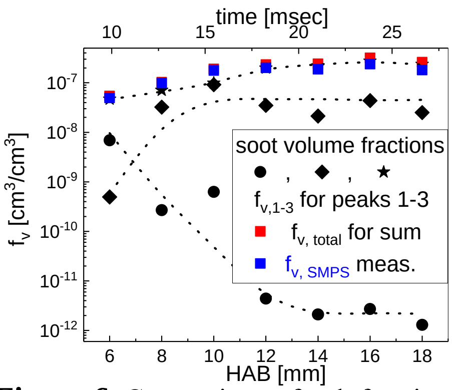

Figure 5. Comparison of particle sizes. **Figure 6.** Comparison of vol. fractions.

Conclusions

A novel peak fitting method has been used to evaluate soot particle size distributions in flat, premixed $CH_4/O_2/Ar$ flames measured by SMPS. The experimental results can be represented very precisely by superposition of three lognormal modes. Even more peaks do not improve the fit precision further. Also, the procedure helps to make plausible estimates of the particle inception mode which is difficult to detect by SMPS. Therefore, the resulting total particle number densities turn out to be significantly higher than determined by SMPS at low HAB (the SMPS intrinsically employs the single peak assumption). This may also help to quantify diffusion losses during the SMPS measurement in the future. The total soot particle volume fractions agree within a ± 30% range. The novel peak fitting method can also be applied to other types of size distributions and, it will also allow better insight into the particle coagulation kinetics in the future.

Acknowledgements

The authors gratefully acknowledge the financial support by Federal Ministry of Food and Agriculture in the project "Formation of soot particles and catalytic filter regeneration for application of biomass fuels in direct-injection spark-ignition engines" (project number: 22040811) and the Helmholtz Association of German Research Centres (HGF).

References

[1] Baukal, C.E., *Oxygen-Enhanced Combustion*, CRC Press, Boca Raton,1998.
[2] Smith, H.C., Pineda, D.I., Ellzey, J.L., "Syngas production from burner-stabilized methane/air flames: The effect of preheated reactants", *Combust. Flame* 160: 557-564 (2013).
[3] Sentko, M., Weis, C., Harth, S., Habisreuther, P., Zarzalis, N., Trimis, D., "Temperature dependency of the laminar burning velocity of fuel-rich

methane oxygen measurements", *Proc. European Combustion Meeting 2015*, Budapest, Hungary, Paper P3-44, March 30–April 2, 2015, (ISBN 978-963-12-1257-0).

[4] Stelzner, B., Weis, C., Habisreuther, P., Zarzalis, N., Trimis, D., "Super-adiabatic flame temperatures in premixed methane flames: A comparison between oxy-fuel and conventional air combustion", *Fuel* 201: 148–55 (2017), doi:10.1016/j.fuel.2017.01.025.

[5] Vlavakis, P., Sentko, M., Loukou, A., Stelzner, B., Trimis D., "Soot formation in premixed fuel-rich oxygen-enhanced methane flames", submitted to Fuel, Dec 2017, manuscript number: JFUE-D-17-04934.

[6] Mätzing, H., Baumann, W., Bockhorn, H., Paur, H.-R., Seifert, H., "Detection of electrically charged soot particles in laminar premixed flames", *Combust. Flame* 159: 1082-1089 (2012).

[7] Zhao, B., Yang, Z., Li, Z., Johnston, M.V., Wang, H., "Particle size distribution function of incipient soot in laminar premixed ethylene flames: effect of flame temperature", *Proc. Comb. Inst.* 30: 1441-1448 (2005).

[8] Maricq, M.M., "Coagulation dynamics of fractal-like soot aggregates", *Aerosol Sci.* 159: 1082-1089 (2012).

[9] Gu, C., Lin, H., Camacho, J., Lin, B., Shao, C., Li, R., Gu, H., Guan, B., Huang, Z., Wang, H., "Particle size distribution of nascent soot in lightly and heavily sooting premixed ethylene flames", *Combust. Flame* 165: 177-187 (2016).

[10] Camacho, J., Singh, A.V., Wang, W., Shan, R., Yapp, E.K.Y., Chen, D., Kraft, M., Wang, H., "Soot particle size distributions in premixed stretch-stabilized flat ethylene–oxygen–argon flames", *Proc. Comb. Inst.* 36: 1001-1009 (2017).

[11] Alderliesten, M., "Mean Particle Diameters. Part VIII. Computer program to decompose mixtures of (truncated) lognormal particle size distributions using differential evolution to generate starting values for nonlinear least squares", *Part. Part. Syst. Charact.* 33: 675-697 (2016).

[12] Herdan, G., Smith, M.L., Hardwick, W.H., Connor, P., *Small particle statistics: an account of statistical methods for the investigation of finely divided materials,* Butterworths, London, 1960.

[13] Price, K.V., Storn, R.M., Lampinen, J.A., *Differential Evolution, A Practical Approach to Global Optimization*, Springer-Verlag, 2005.

[14] DE homepage, http://www1.icsi.berkeley.edu/~storn/code.html (accessed Feb 2018).

[15] Mishra, S.K. (2007), "NLINLS: a Differential Evolution based nonlinear least squares Fortran77 program", http://mpra.ub.uni-muenchen.de/4949/.

[16] Tang, Q., Cai, R., You, X., Jiang, J., "Nascent soot particle size distributions down to 1 nm from a laminar premixed burner-stabilized stagnation ethylene flame", *Proc. Comb. Inst.* 36: 993-1000 (2017).